Electroweak corrections and anomalous triple gauge-boson couplings in W^+W^- and $W^\pm Z$ production at the CERN LHC

E. Accomando[1] and A. Kaiser[2,3]

[1]*Dipartimento di Fisica Teorica, Università di Torino, Via P. Giuria 1, 10125 Torino, Italy*
[2]*Paul Scherrer Institut, CH-5232 Villigen PSI, Switzerland*
[3]*Institute of Theoretical Physics, University of Zürich, CH-8057 Zürich, Switzerland*

(Received 27 March 2006; published 22 May 2006)

We have analyzed the production of WZ and WW vector-boson pairs at the LHC. These processes give rise to four-fermion final states, and are particularly sensitive to possible nonstandard trilinear gauge-boson couplings. We have studied the interplay between the influence of these anomalous couplings and the effect of the complete logarithmic electroweak $\mathcal{O}(\alpha)$ corrections. Radiative corrections to the standard model processes in double-pole approximation and nonstandard terms due to trilinear couplings are implemented into a Monte Carlo program for $pp \to 4f(+\gamma)$ with final states involving four or two charged leptons. We numerically investigate purely leptonic final states and find that electroweak corrections can fake new-physics signals, modifying the observables by the same amount and shape, in kinematical regions of statistical significance.

DOI: 10.1103/PhysRevD.73.093006 PACS numbers: 12.15.Lk

I. INTRODUCTION

In the last few years, LEP2 and Tevatron have provided accurate tests of the non-Abelian structure of the standard model (SM), probing the existence of self-interactions among electroweak gauge bosons. The experimental collaborations have performed several measurements of charged and neutral triple gauge-boson couplings (TGCs), mainly analyzing the production of gauge-boson pairs whose cross sections depend very sensitively on the non-Abelian sector of the underlying theory. Still, up to now the self-couplings have not been determined with the same precision as other boson properties, such as their masses and couplings to fermions. Despite the copious production of W^+W^- pairs at LEP2, the experimental bounds on possible anomalous couplings, which parametrize deviations from SM predictions due to new physics occurring at energy scales of order of tens of TeV, are not very stringent. The weakness of the LEP2 measurement is the rather modest energy scale at which W-pair-production events have been generated. Anomalous gauge-boson couplings are in fact expected to increasingly enhance the gauge-boson pair-production cross section at large di-boson invariant masses $M_{VV'}$ $(V, V' = W, Z, \gamma)$, as they spoil the unitarity cancellations for longitudinal gauge bosons. Hence, at future colliders it will be useful to analyze the di-boson production at the highest possible center-of-mass (CM) energies.

In the near future, the Large Hadron Collider (LHC) will be the main source of vector-boson pairs produced with large invariant mass $M_{VV'}$. The machine will collect hundred thousands of events, the exact statistics depending on the particular process and luminosity [1]. The prospects for a detailed investigation of trilinear couplings will sensibly improve when the envisaged integrated luminosity of 100 fb^{-1} will be reached. Owing to the expected increase in statistics, the measurement of anomalous TGCs requires theoretical predictions from Monte Carlo generators of order of a few percent accuracy to allow for a decent data analysis. At lowest order, this means taking into account spin correlation and finite-width effects, as well as the contribution of the irreducible background coming from all Feynman diagrams which are not mediated by di-boson production but give rise to the same final state. Whenever dominant, these diagrams could spoil the sensitivity to possible new physics, as they do not contain triple gauge-boson couplings. The way to achieve this level of precision is to compute the complete process $pp \to 4f$, going beyond the production $\times$ decay approach. This represents the most basic step towards the desired accuracy. Moreover, a full understanding and control of higher order QCD and electroweak (EW) corrections is necessary to match the experimental error.

In the past years, hadronic di-boson production has been studied extensively by many authors, with particular attention to the $\mathcal{O}(\alpha_s)$ QCD corrections (for a review on the subject see Ref. [1]). Several next-to-leading order (NLO) Monte Carlo programs have been constructed and cross checked so that complete $\mathcal{O}(\alpha_s)$ corrections are now available [2–4]. Inclusive NLO QCD corrections turn out to be very large at LHC energies. They can increase the overall lowest-order cross section by a factor of 2, if no cuts are applied. Their effect is even more pronounced if one considers kinematical distributions particularly sensitive to anomalous couplings. As an example, QCD corrections can increase the tails of vector-boson transverse momentum and di-boson invariant mass distributions by 1 order of magnitude [5,6], thus spoiling the sensitivity to possible deviations from the SM. By including a jet veto, their effects are drastically reduced to the order of tens of percent [2,7], restoring the sensitivity to anomalous WWV couplings.

In view of the envisaged precision of a few percent at the LHC, also a discussion of EW corrections is in order (see, for example, Ref. [8] and references therein). Various analyses of the effect of one-loop logarithmic EW corrections on $W\gamma$, $Z\gamma$, WZ, and WW production processes at the LHC [9–11] have pointed out that $\mathcal{O}(\alpha)$ corrections are comparable or bigger than the statistical error, when exploring large di-boson invariant masses and large rapidity of the produced gauge bosons. This is precisely the kinematical region where effects due to anomalous couplings are expected to be maximally enhanced. Hence, for a meaningful analysis of possible new-physics effects in high-energy domains of suitable distributions, including only universal radiative corrections such as the running of the electromagnetic coupling and corrections to the ρ parameter is not enough. The remaining EW corrections, enhanced by double and single logarithms of the ratio of the CM-energy to the EW scale, may be indeed relevant. The growth of $\mathcal{O}(\alpha)$ EW corrections with increasing energy is well known since a long time. Analyses of the general high-energy behavior of EW corrections have been extensively performed (see for instance Refs. [12,13]). From the computational point of view, a process-independent recipe greatly simplifies the calculation of leading-logarithmic EW corrections. Such a method is described in Refs. [14,15]. There, it has been shown that the leading-logarithmic one-loop corrections to arbitrary EW processes factorize into the tree-level amplitudes times universal correction factors.

Using the method of Refs. [14,15], we have investigated in Ref. [10] the effect of leading-logarithmic $\mathcal{O}(\alpha)$ EW corrections to the hadronic production of $W^{\pm}Z$ and $W^{\pm}W^{\mp}$ pairs in the large-invariant-mass region of the hard process at the LHC. In this paper, we compare their shape and size with the influence of anomalous TGCs on the lowest-order SM predictions. In this study, QCD corrections are not included. The simplest experimental analyses of gauge-boson pair production will rely on purely leptonic final states. Semileptonic channels, where one of the vector bosons decays hadronically, have been analyzed at the Tevatron [16] showing that these events suffer from the background due to the production of one vector boson plus jets via gluon exchange. For this reason, we study only di-boson production where both gauge bosons decay leptonically into e or μ.

The paper is organized as follows: the relevant triple gauge-boson couplings and the parametrization used to calculate their contribution to $pp \to 4f(+\gamma)$ processes are given in Sec. II. The strategy of our calculation, which improves the tree-level predictions by including one-loop electroweak corrections, is described in Sec. III. The general setup of our numerical analysis and the discussion of processes mediated by WZ and WW production are given in Sec. IV. Our findings are summarized in Sec. V.

II. TRIPLE GAUGE-BOSON COUPLINGS

New physics occurring at energy scales much larger than those probed directly at forthcoming experiments could modify the structure of the vector-boson self-interactions. These modifications are parametrized in terms of anomalous couplings in the Yang-Mills vertices. The hadronic production of WW and WZ pairs is sensitive to possible anomalous triple gauge-boson couplings in the charged sector, i.e. to anomalous W^+W^-Z and $W^+W^-\gamma$ couplings.[1] The two most general vertices, which preserve Lorentz invariance and separate C- and P-conservation, are described by the effective Lagrangian suggested in Ref. [17]:

$$\mathcal{L}_{WWV} = g_{WWV}\Big[g_1^V (W^\dagger_{\mu\nu} W^\mu V^\nu - W^\dagger_\mu V_\nu W^{\mu\nu}) + \kappa^V W^\dagger_\mu W_\nu V^{\mu\nu} + \frac{\lambda^V}{M_W^2} W^\dagger_{\rho\mu} W^\mu_\nu V^{\nu\rho} \Big], \quad (2.1)$$

where V^μ represents the Z and γ fields, $X^{\mu\nu} = \partial_\mu X_\nu - \partial_\nu X_\mu$ (for $X = W, Z, \gamma$), $g_{WW\gamma} = -e$, and $g_{WWZ} = e\cot\theta_w$, with θ_w the weak mixing angle and e the electric charge. For simplicity, C- or P-violating WWV couplings are not considered in this paper. The six free parameters in Eq. (2.1) can be written in terms of their deviation, Δ, from the corresponding SM values:

$$g_1^V = 1 + \Delta g_1^V, \qquad \kappa^V = 1 + \Delta\kappa^V, \qquad \lambda^V = \Delta\lambda^V. \quad (2.2)$$

Instead of using rather general parametrizations of non-standard couplings, we adopt a convention commonly used in the LEP2 data analysis [18] to reduce the number of free parameters. We assume in the following that $\Delta g_1^\gamma = 0$. The remaining couplings are further constrained by the relations:

$$\lambda_Z = \lambda_\gamma, \qquad \Delta\kappa_Z = \Delta g_1^Z - \tan^2\theta_w \Delta\kappa_\gamma. \quad (2.3)$$

In this approach, we are thus left with only three independent parameters, i.e. g_1^Z, κ_γ, and λ_γ. LEP2 and Tevatron have constrained the value of the WWV coupling constants at the few-percent level. The experimental average gives the following 95% confidence intervals [19]:

$$-0.054 \le \Delta g_1^Z \le 0.028, \qquad -0.117 \le \Delta\kappa_\gamma \le 0.061, \qquad -0.07 \le \Delta\lambda_\gamma \le 0.012, \quad (2.4)$$

where each parameter has been determined from a single-parameter fit, that is performed by assuming SM values for all other couplings. Taking constant values for the anomalous couplings in the effective Lagrangian (2.1) would violate unitarity. In order to preserve that, any deviation from the SM expectations must be inserted into the vertices

[1] We do not discuss here purely neutral gauge-boson couplings, involving only Z and γ.

via a form factor which vanishes at asymptotically high energies [20]:

$$\Delta' Y = \frac{\Delta Y}{(1+\hat{s}/\Lambda_{FF}^2)^n}, \qquad Y = g_1^Z, \kappa_\gamma, \lambda_\gamma, \tag{2.5}$$

with ΔY the value at low energy, $\sqrt{\hat{s}}$ the partonic CM-energy, and Λ_{FF} the energy scale at which new physics could possibly appear.

At the Born level, it is straightforward to include anomalous couplings in the matrix elements. On the contrary, at one-loop, nonstandard model contributions do not guarantee the renormalizability of the electroweak theory. Consequently, we consider their effect only on the lowest-order cross section.

III. STRATEGY OF THE CALCULATION

We consider the production of massive gauge-boson pairs in proton-proton collisions. In the parton model the corresponding cross sections are described by the following convolution

$$\mathrm{d}\sigma^{h_1 h_2}(P_1, P_2, p_f) = \sum_{i,j} \int_0^1 \mathrm{d}x_1 \int_0^1 \mathrm{d}x_2 \Phi_{i,h_1}(x_1, Q^2) \times \Phi_{j,h_2}(x_2, Q^2) \mathrm{d}\hat{\sigma}^{ij}(x_1 P_1, x_2 P_2, p_f), \tag{3.1}$$

where p_f summarizes the final-state momenta, Φ_{i,h_1} and Φ_{j,h_2} are the distribution functions of the partons i and j in the incoming protons h_1 and h_2 with momenta P_1 and P_2, respectively, Q is the factorization scale, and $\hat{\sigma}^{ij}$ represent the cross sections for the partonic processes averaged over colors and spins of the partons. At lowest order, these cross sections are calculated using the matrix elements for the complete process

$$\bar{q}_1(p_1, \sigma_1) + q_2(p_2, \sigma_2) \to f_3(p_3, \sigma_3) + f_4(p_4, \sigma_4) + f_5(p_5, \sigma_5) + f_6(p_6, \sigma_6), \tag{3.2}$$

where the arguments label momenta p_i and helicities σ_i of the external fermions. This means that we include the full set of Feynman diagrams, in this way accounting for the resonant di-boson production as well as the irreducible background coming from nondoubly resonant contributions. Complete four-fermion phase spaces and exact kinematics are employed in our calculation. For the evaluation of the electroweak corrections we follow the approach developed and described in Refs. [10,21]. Explicit formulas for the processes (3.2) discussed in this paper are given in Ref. [10]. In the following we simply summarize the kernel of the adopted approximations and discuss their applicability domains.

The virtual corrections, coming from loop diagrams, are computed in double-pole approximation (DPA), that is taking into account only those terms which are enhanced by two resonant gauge-boson propagators, $\bar{q}_1 q_2 \to V_1 V_2 \to 4f$. In DPA, the generic process we want to analyze has the structure depicted in Fig. 1. The matrix element factorizes into the production of two on-shell bosons, $\mathcal{M}_{\mathrm{Born}}^{\bar{q}_1 q_2 \to V_{1,\lambda_1} V_{2,\lambda_2}}$, their propagators, and their decay into fermion pairs, $\mathcal{M}_{\mathrm{Born}}^{V_{k,\lambda_k} \to f_i \bar{f}_j}$,

$$\mathcal{M}_{\mathrm{Born,DPA}}^{\bar{q}_1 q_2 \to V_1 V_2 \to 4f} = P_{V_1}(k_1^2) P_{V_2}(k_2^2) \sum_{\lambda_1, \lambda_2} \mathcal{M}_{\mathrm{Born}}^{\bar{q}_1 q_2 \to V_{1,\lambda_1} V_{2,\lambda_2}} \times \mathcal{M}_{\mathrm{Born}}^{V_{1,\lambda_1} \to f_3 \bar{f}_4} \mathcal{M}_{\mathrm{Born}}^{V_{2,\lambda_2} \to f_5 \bar{f}_6}. \tag{3.3}$$

The sum runs over the physical helicities $\lambda_1, \lambda_2 = 0, \pm 1$ of the on-shell projected gauge bosons V_1 and V_2 with momenta k_1 and k_2, respectively. The propagators of the massive gauge bosons

$$P_V(p) = \frac{1}{p^2 - M_V^2 + \theta(p^2) i M_V \Gamma_V}, \quad V = W, Z \tag{3.4}$$

involve besides the masses of the gauge bosons also their widths, which we consider as constant and finite for timelike momenta. In this approximation, the $\mathcal{O}(\alpha)$ virtual corrections are of two types: factorizable and nonfactorizable ones. The former are those that can be associated either to the production or to the decay subprocess. Their matrix elements for the processes $\bar{q}_1 q_2 \to V_1 V_2 \to 4f$ can be written as

$$\begin{aligned}\delta\mathcal{M}_{\mathrm{virt,DPA,fact}}^{\bar{q}_1 q_2 \to V_1 V_2 \to 4f} = P_{V_1}(k_1^2) P_{V_2}(k_2^2) \sum_{\lambda_1, \lambda_2} \{ & \delta\mathcal{M}_{\mathrm{virt}}^{\bar{q}_1 q_2 \to V_{1,\lambda_1} V_{2,\lambda_2}} \times \mathcal{M}_{\mathrm{Born}}^{V_{1,\lambda_1} \to f_3 \bar{f}_4} \mathcal{M}_{\mathrm{Born}}^{V_{2,\lambda_2} \to f_5 \bar{f}_6} \\ & + \mathcal{M}_{\mathrm{Born}}^{\bar{q}_1 q_2 \to V_{1,\lambda_1} V_{2,\lambda_2}} \delta\mathcal{M}_{\mathrm{virt}}^{V_{1,\lambda_1} \to f_3 \bar{f}_4} \times \mathcal{M}_{\mathrm{Born}}^{V_{2,\lambda_2} \to f_5 \bar{f}_6} + \mathcal{M}_{\mathrm{Born}}^{\bar{q}_1 q_2 \to V_{1,\lambda_1} V_{2,\lambda_2}} \\ & \times \mathcal{M}_{\mathrm{Born}}^{V_{1,\lambda_1} \to f_3 \bar{f}_4} \delta\mathcal{M}_{\mathrm{virt}}^{V_{2,\lambda_2} \to f_5 \bar{f}_6} \}, \end{aligned} \tag{3.5}$$

where $\delta\mathcal{M}_{\mathrm{virt}}^{\bar{q}_1 q_2 \to V_{1,\lambda_1} V_{2,\lambda_2}}$, $\delta\mathcal{M}_{\mathrm{virt}}^{V_{1,\lambda_1} \to f_3 \bar{f}_4}$, and $\delta\mathcal{M}_{\mathrm{virt}}^{V_{2,\lambda_2} \to f_5 \bar{f}_6}$

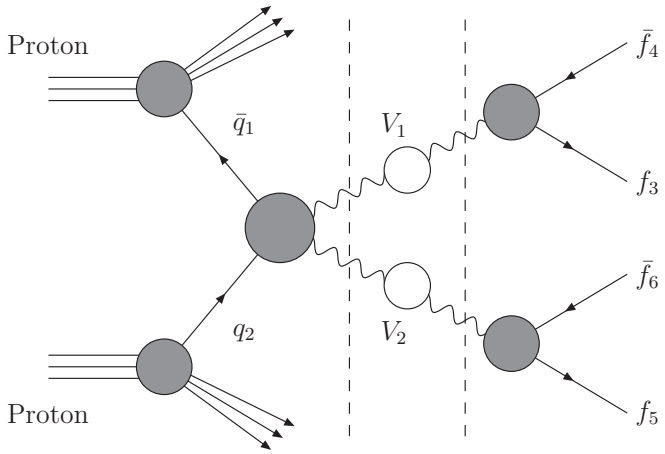

FIG. 1. Structure of the process $pp \to V_1 V_2 + X \to 4f + X$ in DPA.

denote the virtual corrections to the on-shell matrix elements for the gauge-boson production and decay processes. The latter ones connect instead production and decay subprocesses or two decay subprocesses, and yield a simple correction factor $\delta^{\rm virt}_{\rm nf,DPA}$ to the lowest-order cross section.

We calculate factorizable and nonfactorizable $\mathcal{O}(\alpha)$ virtual corrections in logarithmic high-energy approximation, taking into account only contributions involving single and double enhanced logarithms at high energies, i.e. $\mathcal{O}(\alpha)$ contributions proportional to $\alpha\ln^2(|\hat{s}|/M_W^2)$ or $\alpha\ln(|\hat{s}|/M_W^2)$, where $\sqrt{\hat{s}}$ is the CM-energy of the partonic subprocess. The logarithmic approximation yields the dominant corrections as long as CM-energies and scattering angles are large. Pure angular-dependent logarithms of the form $\alpha\ln^2(|\hat{s}|/\hat{r})$ or $\alpha\ln(|\hat{s}|/\hat{r})$, with $\hat{r}$ equal to the Mandelstam variables $\hat{t}$ and $\hat{u}$ of the partonic production subprocess, are in fact not included. The validity of the results relies therefore on the assumption that all invariants are large compared with M_W^2 and approximately of the same size

$$\hat{s} \sim |\hat{t}| \sim |\hat{u}| \gg M_W^2. \tag{3.6}$$

This implies that the produced gauge bosons should be energetic and emitted at sufficiently wide angles with respect to the beam. This is precisely the kinematical region where effects due to possible anomalous couplings should be most enhanced. In this region, the accuracy of the logarithmic high-energy approximation is expected to be of order of a few percent. Numerical estimates of the omitted terms, based on the comparison between complete $\mathcal{O}(\alpha)$ corrections and their high-energy limit for different processes [11,12], confirm this level of precision. We can thus reasonably adopt this approximation at the LHC, where the experimental error in the high-energy regime is at the few-percent level.

The afore-mentioned $\mathcal{O}(\alpha)$ contributions originate from above the EW scale, and affect only the production subprocess. In addition, one has to consider purely electromagnetic logarithmic corrections of the form $\ln(M_W^2/m_f^2)$ or $\ln(M_W^2/\lambda^2)$, where λ is the photon mass regulator and m_f the fermion mass, which originate from below the EW scale. These large logarithms from diagrams with photon exchange affect also the decay subprocesses, giving rise to a correction factor proportional to the lowest-order matrix element [10].

Soft and collinear singularities must be cancelled against their counterparts in the real corrections. Conversely to the virtual corrections, these latter ones are calculated using the matrix elements for the complete processes

$$\begin{aligned}\bar{q}_1(p_1,\sigma_1) + q_2(p_2,\sigma_2) \to\ & f_3(p_3,\sigma_3) + f_4(p_4,\sigma_4)\\ & + f_5(p_5,\sigma_5) + f_6(p_6,\sigma_6)\\ & + \gamma(k,\lambda_\gamma)\end{aligned} \tag{3.7}$$

with emission of an additional photon of momentum k and helicity $\lambda_\gamma = \pm 1$. The well-known phase-space slicing method (see e.g. Ref. [22]) is employed for isolating soft and collinear divergencies. The details of the implementation are given in Ref. [10].

IV. NUMERICAL STUDIES

In this section, we illustrate the impact of the one-loop electroweak radiative corrections on the observability of anomalous triple gauge-boson couplings in WZ and WW production at the LHC. We consider two classes of processes:

(i) $pp \to l\nu_l l'\bar{l}'(+\gamma)$,
(ii) $pp \to l\bar{\nu}_l \nu_{l'}\bar{l}'(+\gamma)$,

where $l, l' = e$ or μ. In our notation, $l\nu_l$ indicates both $l^-\bar{\nu}_l$ and $l^+\nu_l$. The first class is characterized by three isolated charged leptons plus missing energy in the final state. This channel includes WZ production as intermediate state. The second class is instead related to $W^\pm W^\mp$ production. When there is a unique flavor in the final state, $l = l'$, the latter process receives also a ZZ contribution. In the parton model the corresponding cross sections are described by the convolution in Eq. (3.1). Since the two incoming hadrons are protons and we sum over final states which are related one another by charge conjugation, we find

$$\begin{aligned}\mathrm{d}\sigma^{pp}(P_1,P_2,p_f) = \int_0^1 \mathrm{d}x_1\mathrm{d}x_2 \sum_{U=u,c}\sum_{D=d,s} & [\Phi_{\bar{D},p}(x_1,Q^2)\Phi_{U,p}(x_2,Q^2)\mathrm{d}\hat{\sigma}^{\bar{D}U}(x_1P_1,x_2P_2,p_f)\\ & + \Phi_{\bar{U},p}(x_1,Q^2)\Phi_{D,p}(x_2,Q^2)\mathrm{d}\hat{\sigma}^{\bar{U}D}(x_1P_1,x_2P_2,p_f) + \Phi_{\bar{D},p}(x_2,Q^2)\Phi_{U,p}(x_1,Q^2)\mathrm{d}\hat{\sigma}^{\bar{D}U}(x_2P_2,x_1P_1,p_f)\\ & + \Phi_{\bar{U},p}(x_2,Q^2)\Phi_{D,p}(x_1,Q^2)\mathrm{d}\hat{\sigma}^{\bar{U}D}(x_2P_2,x_1P_1,p_f)]\end{aligned} \tag{4.1}$$

for WZ production and

$$\begin{aligned}\mathrm{d}\,\sigma^{pp}(P_1,P_2,p_f) = \int_0^1 \mathrm{d}x_1\mathrm{d}x_2 \sum_{q=u,d,c,s} & [\Phi_{\bar{q},p}(x_1,Q^2)\Phi_{q,p}(x_2,Q^2)\mathrm{d}\hat{\sigma}^{\bar{q}q}(x_1P_1,x_2P_2,p_f)\\ & + \Phi_{\bar{q},p}(x_2,Q^2)\Phi_{q,p}(x_1,Q^2)\mathrm{d}\hat{\sigma}^{\bar{q}q}(x_2P_2,x_1P_1,p_f)]\end{aligned} \tag{4.2}$$

for WW (and ZZ) production in leading order of QCD. In computing partonic cross sections, for the free parameters we use

the input values [23,24]:

$$G_\mu = 1.16637 \times 10^{-5}\ \text{GeV}^{-2}, \qquad M_W = 80.425\ \text{GeV},$$
$$M_Z = 91.1876\ \text{GeV}, \qquad m_t = 178.0\ \text{GeV}. \tag{4.3}$$

The weak mixing angle is fixed by $s_W^2 = 1 - M_W^2/M_Z^2$. Moreover, we adopted the so-called G_μ-scheme, which effectively includes higher-order contributions associated with the running of the electromagnetic coupling and the leading universal two-loop m_t-dependent corrections. To this end we parametrize the lowest-order matrix element in terms of the effective coupling $\alpha_{G_\mu} = \sqrt{2} G_\mu M_W^2 s_W^2/\pi = 7.543\,596\ldots \times 10^{-3}$ and omit the explicit contributions proportional to $\Delta\alpha(M_W^2)$ and $\Delta\alpha(M_Z^2)$ in the electroweak virtual corrections due to parameter renormalization. Additional inputs are the quark-mixing matrix elements whose values have been taken to be $V_{ud} = 0.974$ [25], $V_{cs} = V_{ud}$, $V_{us} = -V_{cd} = \sqrt{1 - |V_{ud}|^2} = 0.226\,548\ldots$, $V_{tb} = 1$, and zero for all other matrix elements. We have moreover used the fixed-width scheme with $\Gamma_Z = 2.505\,044$ GeV and $\Gamma_W = 2.099\,360$ GeV. As to parton distributions, we have chosen CTEQ6M [26] at the following factorization scales:

$$Q^2 = \tfrac{1}{2}(M_W^2 + M_Z^2 + P_T^2(l\nu_l) + P_T^2(l'\bar{l}')) \tag{4.4}$$

and

$$Q^2 = \tfrac{1}{2}(2M_W^2 + P_T^2(l) + P_T^2(l') + P_T^2(\nu\nu')), \tag{4.5}$$

for WZ and WW production processes, respectively, where P_T is the transverse momentum. For final states that allow for two different sets of reconstructed gauge bosons, we choose the average of the corresponding scales from (4.4) and (4.5) if both reconstructed sets pass the cuts. This scale choice appears to be appropriate for the calculation of differential cross sections, in particular, for vector-boson transverse-momentum distributions. It generalizes the scale of Refs. [2,6] to final states with identical particles.

For the experimental identification of the final states to be analyzed, we have implemented a general set of cuts appropriate for LHC, and defined as follows:

(i) charged lepton transverse momentum $P_T(l) > 20$ GeV,
(ii) missing transverse momentum $P_T^{\text{miss}} > 20$ GeV for final states with one neutrino and $P_T^{\text{miss}} > 25$ GeV for final states with two neutrinos,
(iii) charged lepton pseudorapidity $|\eta_l| < 3$, where $\eta_l = -\ln(\tan(\theta_l/2))$, and θ_l is the polar angle of particle l with respect to the beam.

These cuts approximately simulate the detector acceptance. At Born level, they can be directly implemented on the final-state particles. A complication arises at one-loop level. When calculating real-photonic corrections, the emission of an additional real photon must be taken into account. The afore-mentioned acceptance cuts assume a perfect separation of this extra photon from the charged leptons, which is not very realistic. In order to give a description of the final state closer to the experimental situation, we consider the following photon recombination procedure:

(i) Photons with a rapidity $|\eta_\gamma| > 3$ are treated as invisible.
(ii) If the photon is central enough ($|\eta_\gamma| < 3$) and the rapidity-azimuthal-angle separation between charged lepton and photon $\Delta R_{l\gamma} = \sqrt{(\eta_l - \eta_\gamma)^2 + (\phi_l - \phi_\gamma)^2} < 0.1$, then the photon and lepton momentum four-vectors are combined into an effective lepton momentum.[2]
(iii) If the photon is central enough ($|\eta_\gamma| < 3$), the rapidity-azimuthal-angle separation $\Delta R_{l\gamma} > 0.1$, and the photon energy $E_\gamma < 2$ GeV, then the momenta of the photon and of the nearest charged lepton are recombined.
(iv) In all other cases we assume that the photon can be distinguished in the detector and therefore does not contribute to the processes in consideration. This last requirement amounts to a photon veto, as we discard all events with a visible photon.

Let us notice that this recombination procedure differs from the one adopted in Ref. [10]. The results presented in the following sections cannot be therefore directly compared with those of Ref. [10]. After photon recombination, the effective lepton momentum must pass the acceptance cuts for the different processes, and we use effective lepton momenta to define the above-mentioned factorization scales. For the processes considered, we have also implemented further cuts which are described in due time.

In the following sections, we present results for the LHC at CM-energy $\sqrt{s} = 14$ TeV and an integrated luminosity $L = 100\ \text{fb}^{-1}$. We assume a dipole form factor ($n = 2$) with scale $\Lambda_{FF} = 1$ TeV in Eq. (2.5). In order to study the effect of anomalous triple gauge-boson couplings, we perform a single-parameter analysis. We thus vary one of the independent parameters λ_γ, Δg_1^Z, $\Delta\kappa_\gamma$ at a time, keeping the remaining ones at their SM zero value. The considered scenarios are summarized in Table I, for some representative values. The chosen numbers are meant to be a pure

TABLE I. Different scenarios for the single-parameter analysis of the anomalous triple gauge-boson couplings. Letters a and b correspond to positive and negative values, respectively.

Scenario	λ_γ	λ_Z	Δg_1^Z	$\Delta\kappa_\gamma$	$\Delta\kappa_Z$
Born	0	0	0	0	0
$2a/2b$	0	0	± 0.02	0	± 0.02
$3a/3b$	0	0	0	± 0.04	$\mp 0.011\,42$
$4a/4b$	± 0.02	± 0.02	0	0	0

[2] In our simplified analysis, we treat muons like electrons as far as recombination is concerned. In practice, they have to be treated differently [27,28].

sample set. The purpose of this paper is not a realistic and exhaustive analysis of the observability of new-physics effects. The aim is to give evidence on the interplay between nonstandard terms and EW corrections in a realistic context, i.e. taking into account the present anomalous TGCs exclusion limits and the planned LHC potential. Nonetheless, our Monte Carlo could serve as a tool to estimate the full sensitivity of LHC to nonstandard couplings via differential cross section studies and event selections.

A. WZ production

In this section, we study the leptonic processes $pp \to l\nu_l l'\bar{l}'$ with $l, l' = e$ or μ. These final states are relatively background free, and can be mediated by WZ production. Hence, they provide a good testing ground for the trilinear WWZ coupling, once the Z and W bosons are properly reconstructed. We simulate the Z-boson selection by requiring at least one pair of opposite-sign leptons with invariant mass satisfying the cut

$$|M(l'\bar{l}') - M_Z| < 20 \text{ GeV}. \tag{4.6}$$

In order to isolate the W-boson production, we use instead the transverse mass defined as $M_T(l\nu_l) = \sqrt{E_T^2(l\nu_l) - P_T^2(l\nu_l)}$ as the physical quantity to be restricted. In the following, we require

$$M_T(l\nu_l) < M_W + 20 \text{ GeV}. \tag{4.7}$$

At the tree level, the sensitivity of WZ production to nonstandard triple vertices has been studied in detail (see Ref. [1] and references therein). Also the influence of the $\mathcal{O}(\alpha_s)$ QCD corrections on the observability of new-physics effects have been extensively analyzed [1,2,7]. The general finding is that the inclusion of anomalous couplings at the WWZ vertex enhances cross sections and distributions at large values of the partonic CM-energy, as well as at large scattering angles of the outgoing bosons. Previous calculations [9–11] have shown that $\mathcal{O}(\alpha)$ electroweak corrections to the hadronic di-boson production are sizeable in exactly this same region. In the following, we include the EW corrections and discuss their effect in the analysis of the WWZ triple gauge-boson coupling. We define two sample scenarios, both characterized by large energies and scattering angles in the di-boson rest frame. The first scenario is fixed by requiring the transverse momentum of the reconstructed Z boson to be

$$P_T(Z) > 250 \text{ GeV}. \tag{4.8}$$

As a second scenario, we impose the following cut on the transverse momentum of any charged lepton

$$P_T(l) > 70 \text{ GeV}. \tag{4.9}$$

In these two kinematical regions, we choose to investigate four illustrative distributions. We select two energylike distributions, showing the growth with energy of the effects associated to anomalous couplings with respect to SM results,

$P_T^{\max}(l)$: maximal transverse momentum of the three charged leptons,

$E(Z)$: energy of the reconstructed Z boson,

and two angular distributions

$\Delta y(Zl) = y(Z) - y(l)$: rapidity difference between the reconstructed Z boson and the charged lepton coming from the W-boson decay,

$y(Z)$: rapidity of the reconstructed Z boson.

The rapidity is defined from the energy E and the longitudinal momentum P_L by $y = 0.5 \ln((E + P_L)/(E - P_L))$. This latter choice is motivated by a property of the WZ production. In the SM, the lowest-order amplitude of the process $q_1\bar{q}_2 \to WZ$ exhibits the well-known approximate radiation zero at $\cos\theta_Z^* \simeq 0.1(-0.1)$ for W^+Z (W^-Z) production [29]. Here, θ_Z^* is the Z-boson scattering angle with respect to the incoming quark in the di-boson rest frame. Analogously to the radiation zero in $W\gamma$ production, the approximate amplitude zero in WZ production can be observed in the distribution of the rapidity difference $\Delta y(Zl)$. At the LHC, the SM at leading order predicts indeed for this observable a dip located at $\Delta y(Zl) = 0$. Radiative corrections and anomalous triple couplings might both obscure or enhance this lowest-order SM signature. It is thus important to study the interplay between these two contributions.

We start discussing the scenario (4.8). In Fig. 2, we have plotted the four distributions for the full processes $pp \to l\nu_l l'\bar{l}'$ with $l = e$ or μ. In our notation, $l\nu_l$ indicates both $l^-\bar{\nu}_l$ and $l^+\nu_l$, i.e. we sum over the charge-conjugate final states and over all flavors of the leptons coming from the W boson, except τ's. The naming of the legend within each plot refers to Table I. The upper part of Fig. 2 shows the momentum (left) and energy (right) distributions. As one can see, owing to the growth of the nonstandard terms in the amplitude with the CM-energy, the anomalous couplings give large enhancements in the differential cross section at large values of $P_T^{\max}(l)$ and $E(Z)$. The scenarios $2a/2b$ and $4a/4b$, where Δg_1^Z and λ_Z are different from their SM zero values, respectively, give major deviations from the SM results. This is in agreement with the analysis of Ref. [30]. There, it is shown that the associated terms in the amplitude grow in fact with the CM-energy squared. In contrast, the terms proportional to $\Delta\kappa_Z$ grow only with the CM-energy, thus generating smaller effects on the cross section. In this specific case, the curves $3a/3b$ in Fig. 2 are not distinguishable from the SM result at Born level.

The $\mathcal{O}(\alpha)$ EW corrections might have an influence on the sensitivity of $P_T^{\max}(l)$ and $E(Z)$ distributions to triple gauge-boson couplings. They in fact decrease the lowest-order differential cross section by more than 20%. Therefore, Born level results overestimate the background

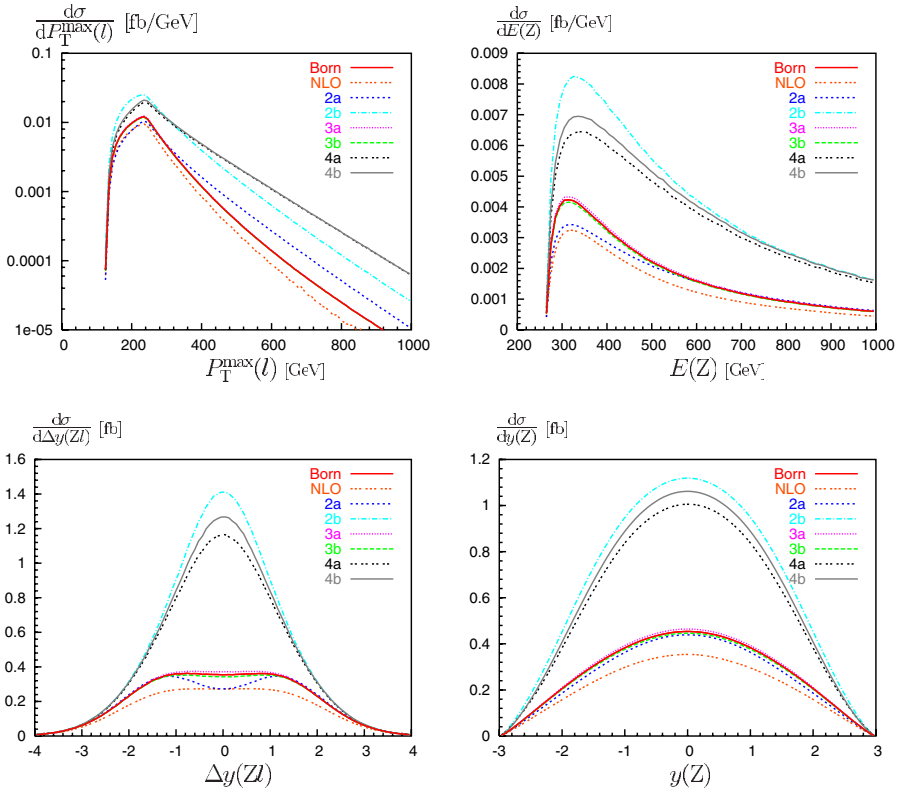

FIG. 2 (color online). Distributions for WZ production. (a) Maximal transverse momentum of the charged leptons. (b) Energy of the reconstructed Z boson. (c) Difference in rapidity between the reconstructed Z boson and the charged lepton coming from the W-boson decay. (d) Rapidity of the reconstructed Z boson. The contributions of the eight final states $l\nu_l l'\bar{l}'$ where $l, l' = e, \mu$ are summed up, and standard cuts as well as $P_T(Z) > 250$ GeV are applied. Legends as explained in the text.

rate, possibly reducing the sensitivity to new-physics effects. An excess of events in the high-energy region could in fact be taken as compatible with the SM predictions, and could therefore be obscured or even missed.

A similar conclusion holds for the two angular distributions shown in the lower part of Fig. 2. The scenarios $2b$ and $4a/4b$ have the largest impact on $\Delta y(Zl)$ and $y(Z)$ variables. In particular, nonzero Δg_1^Z and λ_Z values give rise to enhanced positive contributions and wash out completely the dip of the approximate radiation zero, thus dramatically changing the SM signature. As previously, the $\mathcal{O}(\alpha)$ EW corrections affect the afore-mentioned angular observables by a negative amount of the order of 20%. The distribution in the rapidity difference between the reconstructed Z boson and the charged lepton from the W-boson decay is also suitable to establish the sign of the nonstandard couplings. Assuming a positive value for Δg_1^Z ($2a$ scenario) would generate in fact an opposite effect, actually enhancing the SM dip. Here, the role of the EW radiative corrections might be subtle. They can in fact fake nonstandard Δg_1^Z effects, decreasing the lowest-order $\Delta y(Zl)$ distribution by the same order of magnitude (see the left side lower plot).

The role played by the EW corrections thus depends on the observable and the scenario at hand. Moreover, it can also vary according to the applied kinematical cuts. As an example, if one considers the kinematical region defined by Eq. (4.9), the similarity between $\mathcal{O}(\alpha)$ and nonstandard effects is much more evident. This is shown in Fig. 3 where we plot the same four distributions as before. Here, NLO SM results and $2a$ scenario display the same behavior as compared to the Born SM distributions, independently whether they are energylike or angularlike ($P_T^{\max}(l)$ exhibits this characteristic in the dominant low-value range). The deviation from the lowest-order SM results can reach some tens of percent in both cases, well exceeding the statistical accuracy. The EW corrections should therefore be taken into account to make sure that an experimentally observed discrepancy from the Born SM predictions due to radiative effects is not misinterpreted as a new-physics signal.

The advantage of selecting the less stringent kinematical domain (4.9) consists in roughly doubling the statistics, keeping the good feature of analyzing rather large CM-energies and scattering angles to enhance nonstandard terms. Taking into account all lepton flavors, one has $\sigma_{\text{Born}}(P_T(Z) > 250 \text{ GeV}) = 1.672$ fb and $\sigma_{\text{Born}}(P_T(l) > 70 \text{ GeV}) = 2.64$ fb for scenarios (4.8) and (4.9), respectively. In these two sample regions, the $\mathcal{O}(\alpha)$ corrections have similar consequences on the observability of possible

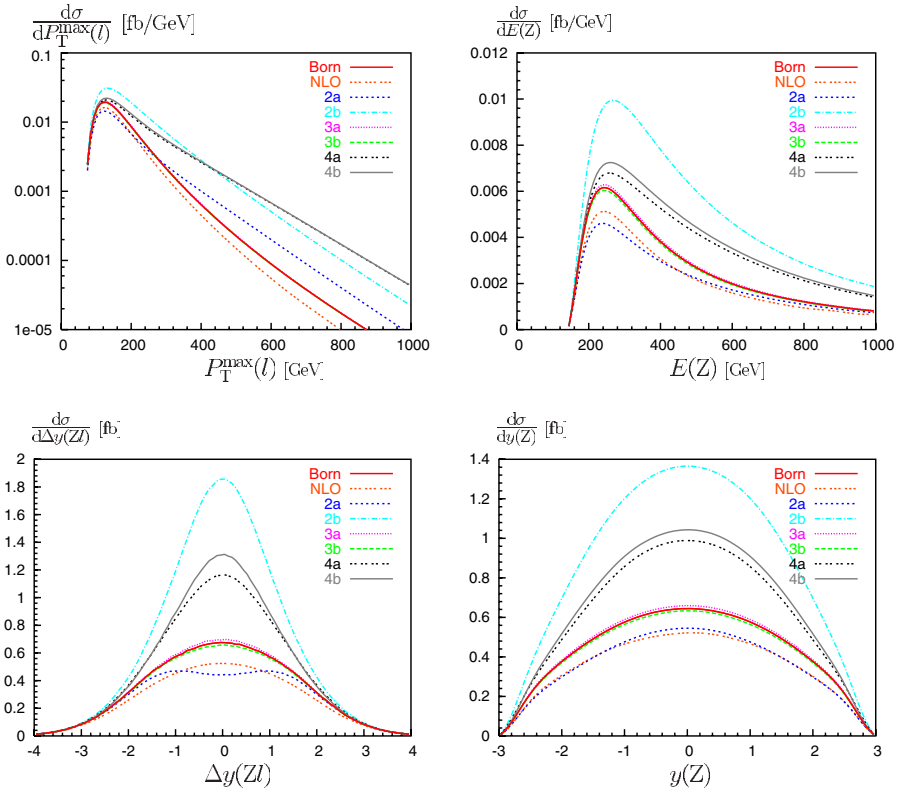

FIG. 3 (color online). Distributions for WZ production. (a) Maximal transverse momentum of the charged leptons. (b) Energy of the reconstructed Z boson. (c) Difference in rapidity between the reconstructed Z boson and the charged lepton coming from the W-boson decay. (d) Rapidity of the reconstructed Z boson. The contributions of the eight final states $l\nu_l l'\bar{l}'$ where $l, l' = e, \mu$ are summed up, and standard cuts as well as $P_T(l) > 70$ GeV are applied. Legends as explained in the text.

new-physics effects. In both cases, they are negative and lower the lowest-order cross section by about 20%.

The significance of the EW corrections can be naively derived from their comparison with the statistical error expected at the LHC. In the low luminosity run, they give a two-standard-deviation effect (2σ) with respect to the Born SM results. In the high luminosity run, their contribution increases up to 4–5σ. The existence of anomalous TGCs might have similar consequences. This is illustrated in more detail in Table II for the scenario (4.8). In columns 3 and 10, we list the relative deviation $\Delta = (\sigma_{\mathrm{NLO}} - \sigma_{\mathrm{Born}})/\sigma_{\mathrm{Born}}$ and the statistical accuracy (estimated by taking as a luminosity $L = 100$ fb^{-1} for two experiments) for some values of the Z-boson transverse momentum cut. We sum over all eight final states $e^-\bar{\nu}_e\mu^-\mu^+$, $\nu_e e^+\mu^-\mu^+$, $\mu^-\bar{\nu}_\mu e^-e^+$, $\nu_\mu\mu^+e^-e^+$, $\mu^-\bar{\nu}_\mu\mu^-\mu^+$, $\nu_\mu\mu^+\mu^-\mu^+$, $e^-\bar{\nu}_e e^-e^+$, $\nu_e e^+e^-e^+$. This comparison indicates that EW corrections can be bigger or comparable with the experimental precision up to about $P_T^{\mathrm{cut}}(Z) = 500$ GeV. In this region the deviation from the Born SM results given by the $\mathcal{O}(\alpha)$ contributions ranges between -23% and -33%. This order of magnitude is much larger or at least comparable with the effect of nonstandard terms coming from $\Delta g_1^Z > 0$ and $\Delta\kappa_\gamma$ (see columns 4, 6, and 7 in Table II). Thus a reliable analysis of the afore-mentioned final states requires the inclusion of the

TABLE II. Cross sections in fb for $pp \to l\nu_l l'\bar{l}'$ where $l, l' = e, \mu$ for different cuts (in GeV) on the transverse momentum of the reconstructed Z boson. All eight final states are summed up, and standard cuts are applied.

$P_T^{\mathrm{cut}}(Z)$	Born	NLO (Δ[%])	$2a$	$2b$	$3a$	$3b$	$4a$	$4b$	$[2L\sigma_{\mathrm{Born}}]^{-1/2}$
250	1.672	1.296 (− 23)	1.576	3.996	1.712	1.644	3.510	3.718	5.5%
300	0.876	0.658 (− 25)	0.940	2.496	0.896	0.862	2.366	2.478	7.6%
350	0.490	0.354 (− 28)	0.606	1.634	0.500	0.482	1.664	1.726	10.1%
400	0.286	0.202 (− 29)	0.410	1.100	0.292	0.284	1.194	1.230	13.2%
450	0.176	0.120 (− 32)	0.286	0.756	0.178	0.174	0.866	0.888	16.9%
500	0.110	0.074 (− 33)	0.202	0.526	0.112	0.110	0.630	0.644	21.3%

$\mathcal{O}(\alpha)$ EW corrections. This kind of accuracy is advisable also in a low luminosity run.

B. *WW* production

In this section, we discuss the processes $pp \to l\bar{\nu}_l \bar{l}' \nu_{l'}$ ($l, l' = e$ or μ). This channel contains informations on the charged gauge-boson vertices, WWZ and $WW\gamma$. It can count on the largest cross section among all massive vector-boson pair-production processes at the LHC, which makes it a favorable channel. Even if it does not allow for a clean and unambiguous reconstruction of the two W bosons, owing to the presence of two neutrinos, it is suitable for measuring triple anomalous couplings. Its goodness depends also on the control one can have on the large background from $t\bar{t}$ production.

We consider the following scenario:

$$M_{\text{inv}}(l\bar{l}') > 500 \text{ GeV}, \qquad |\Delta y_{l\bar{l}'}| < 3. \tag{4.10}$$

Possible ZZ intermediate states are heavily suppressed by the invariant-mass cut in (4.10). Therefore, we can safely neglect the contributions of $e^- e^+ \nu_i \bar{\nu}_i$ ($i = \mu, \tau$) and $\mu^- \mu^+ \nu_i \bar{\nu}_i$ ($i = e, \tau$) final states. We also do not include $\mathcal{O}(\alpha)$ corrections to the ZZ intermediate state contributing to the mixed channels $pp \to e^- e^+ \nu_e \bar{\nu}_e$ and $pp \to \mu^- \mu^+ \nu_\mu \bar{\nu}_\mu$.

For WW production, we choose to discuss distributions in the following variables:

$P_T^{\max}(l)$: maximal transverse momentum of the two charged leptons,

$\Delta y(l\bar{l}')$: rapidity difference between the two charged leptons,

$E(W^+)$: energy of the W^+ boson,

$y(W^-)$:] rapidity of the W^- boson.

Despite the fact that we do not perform a reconstruction of the two W bosons, the last two unphysical distributions are useful to display some peculiarities of EW corrections and anomalous couplings. In Fig. 4 we show the four distributions for the final states $l\bar{\nu}_l \bar{l}' \nu_{l'}$ ($l, l' = e$ or μ), with our standard cuts applied. The general behavior of the EW corrections does not present novelties compared to the previous case. As for WZ production, $\mathcal{O}(\alpha)$ corrections are in fact enhanced at high CM-energies and large scattering angles. This translates into larger radiative effects in the tail of transverse momentum and energy distributions, and in the central region of rapidity distributions, as shown in the two upper and lower plots of Fig. 4, respectively.

The interest in WW processes is twofold. The main feature is the remarkable statistics of purely leptonic final

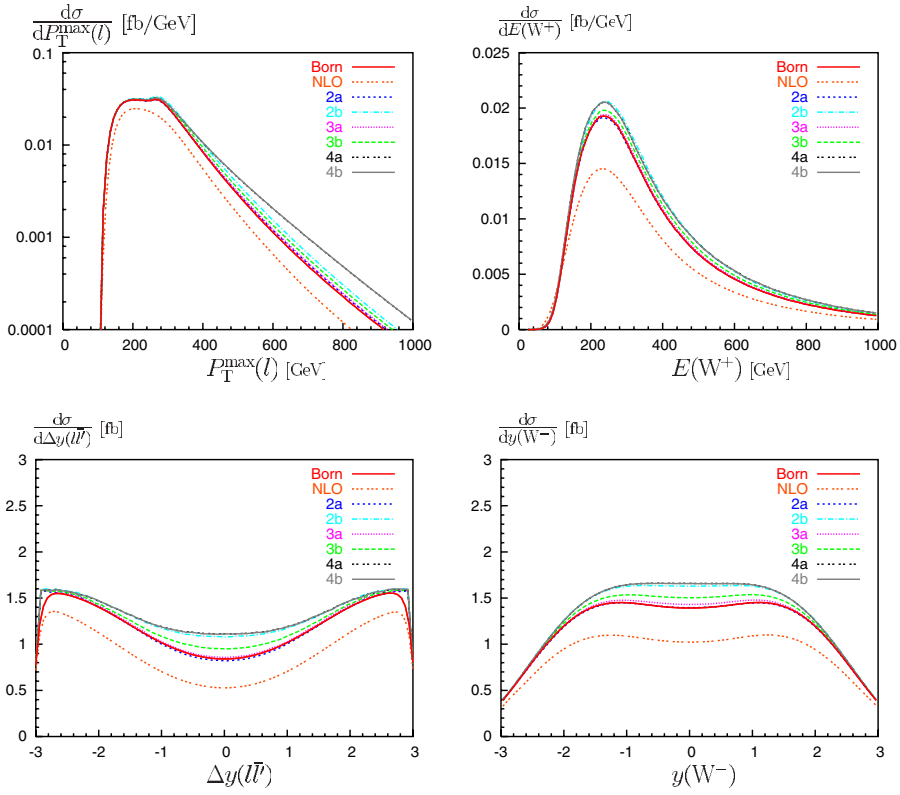

FIG. 4 (color online). Distributions for WW production. (a) Maximal transverse momentum of the charged leptons. (b) Energy of the W boson. (c) Rapidity difference of the two charged leptons. (d) Rapidity of the W^- boson. The contributions of the four final states $l\bar{\nu}_l \nu_{l'} \bar{l}'$ where $l, l' = e, \mu$ are summed up, and standard cuts as well as $M_{\text{inv}}(l\bar{l}') > 500$ GeV and $|\Delta y_{l\bar{l}'}| < 3$ are applied. Legends as explained in the text.

TABLE III. Cross sections in fb for $pp \to l\bar{\nu}_l \nu_{l'} \bar{l}'$ where $l, l' = e, \mu$. All four final states are summed up, and standard cuts as well as $M_{\rm inv}(l\bar{l}') > 500$ GeV and $|\Delta y_{l\bar{l}'}| < 3$ are applied.

$M_{\rm inv}^{\rm cut}(l\bar{l}')$	Born	NLO ($\Delta[\%]$)	$2a$	$2b$	$3a$	$3b$	$4a$	$4b$	$[2L\sigma_{\rm Born}]^{-1/2}$
500	7.239	5.559 ($-$ 23)	7.222	7.978	7.351	7.587	8.026	8.024	2.6%

states. As shown in Table III, where we sum over the four final states $e^-\bar{\nu}_e\nu_\mu\mu^+$, $\nu_e e^+\mu^-\bar{\nu}_\mu$, $\mu^-\bar{\nu}_\mu\nu_\mu\mu^+$, and $e^-\bar{\nu}_e\nu_e e^+$, the estimated experimental precision is around a few percent at CM-energies above 500 GeV. The second characteristic is the stronger interplay between EW corrections and anomalous coupling effects. Both total cross sections (see Table III) and distributions exhibit a poor sensitivity to nonstandard terms in WWZ and $WW\gamma$ vertices. The major effects are obtained when the interference between anomalous contributions and large SM amplitudes can be exploited. Unfortunately, the W-boson pair production is dominated by the Feynman diagram with t-channel neutrino exchange, which does not involve TGCs. The interesting interferences are thus suppressed [31]. As a result, when looking at the total cross section, the effect is at most of order 10% if compared to the lowest-order SM predictions. It slightly increases in some particular distributions.

The optimal case would be considering observables related to the intermediate gauge bosons. As shown in the right side lower plot of Fig. 4, the anomalous couplings influence mostly those events where the W's are produced at large angles with respect to the beam. Unfortunately, for purely leptonic final states, gauge-boson variables are not physical as the W's cannot be reconstructed. One has to resort to observables related to the two charged leptons in order to find out a measurable effect. This indirect detection of the gauge-boson properties might in principle deplete the effective strength of the nonstandard terms. Selecting appropriate variables, like the rapidity difference between the two charged leptons shown in the left side lower plot of Fig. 4, their effect can be preserved. Here, however, the deviation from the SM result is at most of the order of 40%, and it is concentrated around the dip where the events are less abundant. The situation slightly improves if one looks at the distribution in the maximum transverse momentum of the two charged leptons. Analogous results are obtained for the distribution in the transverse momentum of the charged lepton pair. This observable has been investigated in a more general setup in Ref. [32], and found to be particularly sensitive to anomalous couplings. Also for this promising variable, in our single-parameter analysis where we consider smaller deviations from SM couplings and switch on simultaneously the anomalous γWW and ZWW contributions, sizeable effects appear in regions of moderate statistics.

On the other side, in the same energy domain as defined by (4.10), the impact of the $\mathcal{O}(\alpha)$ contributions is of much greater significance. If one considers the total cross section, it amounts to about -23% of the lowest-order result (see Table III). For the chosen setup, this means a 8σ effect which is more than a factor two larger than that generated by nonstandard scenarios. The distributions plotted in Fig. 4 confirm this behavior. The $\mathcal{O}(\alpha)$ effects are in fact shown to be generally bigger than those ones due to possible new physics. Thus, for any decent analysis of the afore-mentioned final states, Monte Carlo programs should include the electroweak radiative effects.

V. CONCLUSIONS

We have explored some aspects of gauge-boson physics at the LHC, i.e. the influence of nonstandard trilinear gauge-boson couplings on WZ and WW di-boson production. To this aim, we have analyzed two classes of processes $pp \to l\nu_l l'\bar{l}'$ and $pp \to l\bar{\nu}_l\nu_{l'}\bar{l}'$, which contain WZ and WW pairs as intermediate state, respectively, and provide a rather clean leptonic signature. We have examined these processes in the physically relevant region of high di-boson invariant mass and large vector-boson scattering angle, where effects due to anomalous TGCs are expected to be maximally enhanced.

In our analysis, we have employed a complete four-fermion calculation, taking into account the decays of the gauge bosons as well as the irreducible background coming from all not double-resonant Feynman diagrams which give rise to the same final state. The primary aim of our study was to understand the interplay between the effect due to anomalous TGCs and the influence of electroweak radiative corrections. Both contributions to the di-boson production processes are enhanced in the kinematical domain of interest. We have thus compared cross sections and distributions obtained for different anomalous TGC parameters with the results predicted by the standard model, including full $\mathcal{O}(\alpha)$ electroweak corrections. The one-loop radiative corrections to the complete four-fermion processes have been evaluated in double-pole approximation, and keeping leading-logarithmic terms of the ratio $\sqrt{\hat{s}}/M_W$ between CM-energy and EW scale. In this approximation, the $\mathcal{O}(\alpha)$ contribution is split into corrections to the gauge-boson-pair-production subprocesses, corrections to the gauge-boson decays, and nonfactorizable corrections. We have also included the full electromagnetic logarithmic corrections, which involve the emission of real photons and thus depend on the detector resolution.

In order to illustrate the behavior and the size of the nonstandard TGC contributions as compared to the $\mathcal{O}(\alpha)$ effects, we have presented various cross sections and dis-

tributions. The comparison shows clearly that the EW corrections can be of the same order of magnitude and shape as the contributions from the anomalous couplings. In the sample scenarios we considered, the $\mathcal{O}(\alpha)$ contributions decrease the lowest-order SM results by 23%–33%. Their impact thus well exceeds the few-percent-order statistical error envisaged at the LHC.

As for the majority of the anomalous TGC parameters the nonstandard terms lead to an increase of the SM results, the inclusion of the EW corrections improves the sensitivity to possible new physics by correcting the overestimation of the SM background. In an opposite way, when nonstandard terms manifest themselves in a decrease of the lowest-order results, the $\mathcal{O}(\alpha)$ corrections may instead fake anomalous contributions. In this case, a pure SM radiative effect could be misinterpreted as a new-physics signal. The EW radiative effects should therefore be taken into account in measuring the $WW\gamma$ and WWZ vertices at the LHC. This conclusion is not peculiar of foreseen high luminosities, but applies also to the initial low luminosity run.

Although, the logarithmic high-energy approximation gives a good and reliable estimate of the EW radiative effects up to a few-percent accuracy, the large statistics of di-boson events at the LHC pushes towards an even higher precision. Along this direction, there is still much to do. Computing full $\mathcal{O}(\alpha)$ corrections would be highly desirable. A first calculation in leading-pole approximation has been performed for $W\gamma$ and $Z\gamma$ processes [11], showing a difference of about 5% compared to the approximate results [10]. Moreover, in the large di-boson invariant-mass region, of interest for EW measurements and new-physics searches, the growth of the Sudakov logarithmic terms is so sharp that they have to be resummed. Although the resummation of these leading effects has been largely discussed on a general basis for four-fermion EW processes, such a calculation has not been carried out yet for any specific di-boson production process.

In order to cope with the envisaged precision of the LHC, fixed-order one-loop corrections and resummation of leading terms should be considered. Having under control QCD and EW corrections, the final aim should be a calculation which combines QCD and EW radiative effects. If a jet veto is imposed, QCD and EW corrections are comparable in size, giving rise to subtle effects of radiative enhancement or balance. Taking into account their interplay would give the most accurate and complete theoretical predictions to fully exploit the LHC potential for EW measurements in di-boson processes.

ACKNOWLEDGMENTS

A. Denner is gratefully acknowledged for extensive discussions on the subject treated and for carefully reading the manuscript. We also thank G. Passarino for valuable comments. This work was supported by the Italian Ministero dell'Istruzione, dell'Università e della Ricerca (MIUR) under Contract Decreto MIUR 26-01-2001 N.13 "Incentivazione alla mobilità di studiosi stranieri ed italiani residenti all'estero."

[1] S. Haywood, P. R. Hobson, W. Hollik, Z. Kunszt *et al.*, CERN Report No. CERN-2000-004, Genève, 2000, p. 117, edited by G. Altarelli and M. L. Mangano (to be published).
[2] L. Dixon, Z. Kunszt, and A. Signer, Phys. Rev. D **60**, 114037 (1999).
[3] D. De Florian and A. Signer, Eur. Phys. J. C **16**, 105 (2000).
[4] J. M. Campbell and R. K. Ellis, Phys. Rev. D **60**, 113006 (1999).
[5] J. Ohnemus, Phys. Rev. D **44**, 3477 (1991).
[6] S. Frixione, P. Nason, and G. Ridolfi, Nucl. Phys. **B383**, 3 (1992).
[7] U. Baur, T. Han, and J. Ohnemus, Phys. Rev. D **51**, 3381 (1995).
[8] W. Hollik *et al.*, Acta Phys. Pol. B **35**, 2533 (2004).
[9] E. Accomando, A. Denner, and S. Pozzorini, Phys. Rev. D **65**, 073003 (2002); W. Hollik and C. Meier, Phys. Lett. B **590**, 69 (2004).
[10] E. Accomando, A. Denner, and A. Kaiser, Nucl. Phys. **B706**, 325 (2005); A. Kaiser, University Zürich 2004 (unpublished).
[11] E. Accomando, A. Denner, and C. Meier, hep-ph/0509234.
[12] W. Beenakker *et al.*, Nucl. Phys. **B410**, 245 (1993).
[13] M. Beccaria, G. Montagna, F. Piccinini, F. M. Renard, and C. Verzegnassi, Phys. Rev. D **58**, 093014 (1998); P. Ciafaloni and D. Comelli, Phys. Lett. B **446**, 278 (1999); J. H. Kühn and A. A. Penin, hep-ph/9906545; M. Beccaria, P. Ciafaloni, D. Comelli, F. Renard, and C. Verzegnassi, Phys. Rev. D **61**, 073005 (2000); V. S. Fadin, L. N. Lipatov, A. D. Martin, and M. Melles, Phys. Rev. D **61**, 094002 (2000); W. Beenakker and A. Werthenbach, Phys. Lett. B **489**, 148 (2000); Nucl. Phys. **B630**, 3 (2002); J. Layssac and F. M. Renard, Phys. Rev. D **64**, 053018 (2001); M. Melles, Phys. Rep. **375**, 219(2003); J. H. Kühn *et al.*, Nucl. Phys. **B616**, 286 (2001); **B648**, 455(E) (2003); M. Beccaria, F. M. Renard, and G. Verzegnassi, Nucl. Phys. **B663**, 394 (2003); S. Pozzorini, Nucl. Phys. **B692**, 135 (2004); B. Feucht, J. H. Kühn, A. A. Penin, and V. A. Smirnov, Phys. Rev. Lett. **93**, 101802(2004).
[14] A. Denner and S. Pozzorini, Eur. Phys. J. C **18**, 461 (2001).
[15] A. Denner and S. Pozzorini, Eur. Phys. J. C **21**, 63 (2001).

[16] F. Abe *et al.* (CDF Collaboration), Phys. Rev. Lett. **75**, 1017 (1995); F. Abachi *et al.* (D0 Collaboration), Phys. Rev. Lett. **77**, 3303 (1996); **79**, 1441 (1997).
[17] K. Hagiwara, R. D. Peccei, D. Zeppenfeld, and K. Hikasa, Nucl. Phys. **B282**, 253 (1987).
[18] G. Gounaris *et al.*, in CERN Report No. CERN 96-01, Vol. 1, p. 525, edited by G. Altarelli, T. Sjöstrand, and F. Zwirner (to be published).
[19] S. Eidelman *et al.*, Phys. Lett. B **592**, 1 (2004); 2005 partial update for the 2006 edition available on the PDG WWW pp. (URL: http://pdg.lbl.gov/).
[20] U. Baur and D. Zeppenfeld, Phys. Lett. B **201**, 383 (1988); Nucl. Phys. **B308**, 127 (1988).
[21] A. Denner, S. Dittmaier, M. Roth, and D. Wackeroth, Nucl. Phys. **B587**, 67 (2000).
[22] F. A. Berends, R. Kleiss, P. De Causmaecker, R. Gastmans, W. Troost, and T. T. Wu, Nucl. Phys. **B206**, 61 (1982); R. Kleiss, Z. Phys. C **33**, 433 (1987).
[23] K. Hagiwara *et al.* (Particle Data Group Collaboration), Phys. Rev. D **66**, 010001 (2002).
[24] CDF Collaboration, D0 Collaboration, Tevatron Electroweak Working Group, hep-ex/0404010.
[25] A. Höcker, H. Lacker, S. Laplace, and F. Le Diberder, Eur. Phys. J. C **21**, 225 (2001).
[26] J. Pumplin, D. R. Stump, J. Huston, H. L. Lai, P. Nadolsky, and W. K. Tung, J. High Energy Phys. 07 (2002) 012.
[27] U. Baur and D. Wackeroth, Phys. Rev. D **70**, 073015 (2004).
[28] A. Airapetian *et al.* (ATLAS Collaboration), CERN Report No. CERN-LHCC-99-14 (unpublished).
[29] U. Baur, T. Han, and J. Ohnemus, Phys. Rev. Lett. **72**, 3941 (1994).
[30] H. Aihara *et al.*, hep-ph/9503425.
[31] D. Zeppenfeld, hep-ph/9506239.
[32] U. Baur, T. Han, and J. Ohnemus, Phys. Rev. D **53**, 1098 (1996).